# NUCLEAR STRUCTURE OF $^{182,184}$Hg ISOTOPES BY IBM-1 AND IBM-2 MODELS

## ESTRUCTURA NUCLEAR DE LOS ISÓTOPOS $^{182,184}$Hg MEDIANTE LOS MODELOS IBM-1 E IBM-2

**Mahdi J. S. Al Musawi[1], Rabee. B. Alkhayat[2], Huda H. Kassim[3], Asmaa A. Elbndag[4], Mushtaq A. Al-Jubbori[2*], I. Hossain[5], Fadhil I. Sharrad[3,6], N. Aldahan[3,6]**

[1] University of Kerbala, College of Medicine, Department of Medical Physics, Karbala, Iraq.
[2] University of Mosul, College of Education for Pure Sciences, Department of Physics, Mosul, Iraq.
[3] University of Kerbala, College of Science, Department of Physics, Karbala, Iraq.
[4] General Department Medical Science and Technology Collage, Tripoli, Libya.
[5] King Abdulaziz University, Rabigh College of Science & Arts, Department of Physics, Rabigh, Saudi Arabia.
[6] University of Alkafeel, College of Health and Medical Technology, Iraq.

(Recibido: aug./2024. Aceptado: jan./2025)

**Abstract**

The potential energy surface (PES), reduced transition strength $B(E2)$, and three types of bands ($g$-band, $\gamma$-band, and $\beta$-band) were computed for the $^{182}$Hg and $^{184}$Hg nuclei employing the IBM-1 and IBM-2 models. The computed energy levels of these nuclei exhibit certain points of agreement with the data that were previously measured. An examination of experimental data reveals that the precision of the calculations performed by IBM-1 is preferable to that of IBM-2, specifically with regard to low energy levels of ground and $\gamma$-states. On the contrary, IBM-2 calculations depict the higher states of ground and other states in comparison to IBM-1. The strengths of quadrupole electromagnetic transitions in these nuclei were established by the IBM-1 and IBM-2 models and compared with prior measured data. The experimental value of $B(E2)$ is reproduced by IBM-2 more accurately than IBM-1. IBM-1

* mushtaq_phy@uomosul.edu.iq doi: https://doi.org/10.15446/mo.n70.116188

is used to analyze the potential energy surfaces (PES) of $^{182,184}$Hg nuclei, which exhibit SU(3)-O(6) dynamical symmetry.

**Keywords:** IBM-1, IBM-2, energy level, $B(E2)$, potential energy, $^{182}$Hg, $^{184}$Hg.

**Resumen**

La superficie de energía potencial (PES), la fuerza de transición reducida $B(E2)$ y tres tipos de bandas (banda $g$, banda $\gamma$, y banda $\beta$) se calcularon para los núcleos $^{182}$Hg y $^{184}$Hg utilizando los modelos IBM-1 e IBM-2. Los niveles de energía calculados de estos núcleos muestran ciertos puntos de concordancia con los datos previamente medidos. Un análisis de los datos experimentales revela que la precisión de los cálculos realizados con IBM-1 es superior a la de IBM-2, específicamente con respecto a los niveles de energía bajos del estado base y los estados $\gamma$. Por el contrario, los cálculos con IBM-2 representan mejor los estados más altos del estado base y otros estados en comparación con IBM-1. Las intensidades de las transiciones electromagnéticas cuadrupolares en estos núcleos se determinaron con los modelos IBM-1 e IBM-2 y se compararon con datos experimentales previos. El valor experimental de $B(E2)$ es reproducido por IBM-2 con mayor precisión que por IBM-1. IBM-1 se utiliza para analizar las PES de los núcleos $^{182,184}$Hg, que exhiben simetría dinámica SU(3)-O(6).

**Palabras clave:** IBM-1, IBM-2, nivel de energía, $B(E2)$, energía potencial, $^{182}$Hg, $^{184}$Hg.

## 1. Introduction

The Interacting Boson Model (IBM-1) is used to deliberate the unified properties of even-even medium-mass nuclei, and the nucleons are not distinguished. However, in IBM-2, the nucleons are distinguished from the closed shells [1, 2]. IBM-1 contains three

types of transitions: vibrational U(5), $\gamma$-soft O(6), and rotational SU(3) symmetry. However, some nuclei may have intermediate structures with U(5)-O(6), U(5)-SU(3), and SU(3)-O(6) symmetry [3, 4]. The infinitesimal source of quadrupole collectivity and shape coexistence at low excitation state in mid-shell nuclei near the double magic nuclei of $^{208}$Pb (Z = 82 and N = 126) shell closures is not yet completely recognized. A considerable proportion of nuclei in the region containing medium-heavy and heavy nuclei display characteristics that are inconsistent with deformed rotors or anharmonic quadrupole vibrational spectra [5]. Low-lying excited states correspond to multiparticle-multihole excitations, as proposed by the nuclear shell model [6–8]. This case regards to lead-region neutron-deficient nuclei (Z = 82). The excited $0^+$ energies decrease as the residual interaction between valence nucleons increases. The extent of this effect is greatest in the region of the neutron center shell (N = 104) [8]. The second $0^+$ energy level exhibits a pronounced decrease in magnitude with the neutron number, occurring at roughly $^{188}$Hg and reaching the midpoint of the main shell at N = 104. The excited energy of $0_2^+$ state drops to roughly $^{182}$Hg before increasing from $^{180}$Hg to $^{178}$Hg. In $^{172,174,176}$Hg, the ground energy levels of $2^+$, $4^+$, and $6^+$ states increase significantly, signifying a shift to spherical vibrational phases [9].

Due to the complicated nature of these nuclear structures and the fact that each nucleon interacts with other nucleons, diagonalizing the transitional Hamiltonian requires the use of sophisticated numerical techniques. The enhancements of the nuclear structure of even neutron-deficient in $^{182,184}$Hg nuclei are very few and hardly found in the literature. The coexistence of neutron-deficient $^{182,184}$Hg nuclei explores lifetime measurements by Siciliano et al. [10]. The triaxial deformation energy surfaces were found to coexist in a configuration of $^{190}$Hg [11]. The work of García-Romas et al. [12] explained the even-even $^{182-190}$Hg isotopes using IBM and configuration mixing. They paid close attention to describing the shape of the nuclei and how it related to the shape-synchronicity phenomenon. Nomura et al. [13] investigated the characteristics of the $^{174–204}$Hg nuclei at lower energy levels. They identified the

shift from a spherical vibrational state at $^{172}$Hg to a spherical vibrational structure near the $^{204}$Hg nucleus. Fortune [14] uses the two mixing state model for 0 and 2 transition elements in $^{182,184}$Hg. He showed that the two states mix in both isotopes, and potential matrix elements do not depend on spin ($j$). The internal conversion coefficients and branching ratios were studied experimentally for excited states in Hg nuclei and interpreted with five different models [15]. The nuclear structure of different types of bands, the $B(E2)$ strength, and the potential energy surfaces (PES) for the $^{182,184}$Hg nuclei based on IBM-1 and IBM-2 models were investigated and compared to existing theoretical calculations. The systematic incentive of the current effort is required to explore the phenomenological properties of the IBM-1 and IBM-2 to explain previously measured results for the nature of three types of energy bands, $B(E2)$, and EPS for the selected nucleus.

## 2. Theoretical framework

### 2.1. IBM-1 and IBM-2 formalisms

The IBM-1 Hamiltonian ($H$) is stated as [16–18]

$$\begin{aligned} H =& \varepsilon_s\big(s^\dagger \cdot \tilde{s}\big) + \varepsilon_d\big(d^\dagger \cdot \tilde{d}\big) \\ &+ \sum_{L=0,2,4} \sqrt{\frac{2L+1}{2}}\, C_L \big[\big[d^\dagger \times d^\dagger\big]^{(L)} \times \big[\tilde{d} \times \tilde{d}\big]^{(L)}\big]^{(0)} \\ &+ \frac{1}{\sqrt{2}}\,\nu_2\big[\big[d^\dagger \times d^\dagger\big]^{(2)} \times \big[\tilde{d} \times \tilde{s}\big]^{(2)} + \big[d^\dagger \times s^\dagger\big]^{(2)} \times \big[\tilde{d} \times \tilde{d}\big]^{(2)}\big]^{(0)} \\ &+ \frac{1}{2}\,\nu_0\big[\big[d^\dagger \times d^\dagger\big]^{(0)} \times \big[\tilde{s} \times \tilde{s}\big]^{(0)} + \big[\big[s^\dagger \times s^\dagger\big]^{(0)} \times \big[\tilde{d} \times \tilde{d}\big]^{(0)}\big]^{(0)} \\ &+ \frac{1}{2}\,u_0\big[\big[s^\dagger \times s^\dagger\big]^{(0)} \times \big[\tilde{s} \times \tilde{s}\big]^{(0)}\big]^{(0)} \\ &+ u_2\big[\big[d^\dagger \times s^\dagger\big]^{(2)} \times \big[\tilde{d} \times \tilde{s}\big]^{(2)}\big]^{(0)}. \end{aligned} \tag{1}$$

Overall, Eq. 1 can also be stated as [19–21]

$$\hat{H} = \varepsilon \hat{n}_d + a_0 \hat{P} \cdot \hat{P} + a_1 \hat{L} \cdot \hat{L} + a_2 \hat{Q} \cdot \hat{Q} + a_3 \hat{T}_3 \cdot \hat{T}_3 + a_4 \hat{T}_4 \cdot \hat{T}_4. \tag{2}$$

$\varepsilon$ is boson energy, $\hat{n}_d$ is the total number of d-bosons, as [22].

$$\hat{n}_d = d^\dagger \cdot (\tilde{d}), \tag{3}$$

the pairing operator is

$$\hat{P} = 0.5 \left[ (\tilde{d} \cdot \tilde{d}) - (\tilde{s} \cdot \tilde{s}) \right], \tag{4}$$

the angular momentum operator is given as

$$\hat{L} = \sqrt{10} \left[ d^\dagger \times \tilde{d} \right]^{(1)}, \tag{5}$$

and the quadrupole operator is [23].

$$\hat{Q} = \left[ d^\dagger \times \tilde{s} + s^\dagger \times \tilde{d} \right]^{(2)} + \chi \left[ d^\dagger \times \tilde{d} \right]^{(2)} \tag{6}$$

The hexadecapole and octupole operators ($\hat{T}_r$) for $r = 4$ and 3 are written as

$$\hat{T}_r = \left[ d^\dagger \times \tilde{d} \right]^{(r)}. \tag{7}$$

The $E2$ transition operator defines [24].

$$T(E2) = \alpha_2 \left[ d^\dagger s + s^\dagger d \right]^{(2)} + \beta_2 \left[ d^\dagger d \right]^{(2)}. \tag{8}$$

The $B(E2)$ is used to understand the decay properties of a nucleus. The PHINT [25] code was used to calculate the $B(E2)$ data as follows:

$$B(E2 : 2_1^+ \to 0_1^+) = \frac{\alpha_2^2}{5} N(N+4) = \frac{e_B^2}{5} N(N+4). \tag{9}$$

Where $e_B$ is effective charge.

It has been proposed that the effective interactions between protons and neutrons tend to induce deformation, whereas the interactions between neutron-neutron and proton-proton exhibit a spherical characteristic [26, 27]. The IBM-2 formalism, an alternative approach to determining the Hamiltonian, is used in this study. In calculating the IBM-2 Hamiltonian, explicit consideration is given to the degrees of freedom of protons and neutrons. One of

its benefits is that it approaches a theory on a microscopic scale. Conversely, the matrices requiring diagonalization are considerably more extensive. Furthermore, the IBM-1 model space can be considered a subspace of the IBM-2 model space [1, 2]. In IBM-2, the $H$ can be expressed as [28].

$$H = \varepsilon_\pi \hat{n}_{d_\pi} + \varepsilon_\nu \hat{n}_{d_\nu} + \kappa Q_\pi \cdot Q_\nu + V_{\pi\pi} + V_{\nu\nu} + M_{\pi\nu}, \tag{10}$$

here $\varepsilon_\nu$, $\varepsilon_\pi$ are the neutron and proton energies, respectively. Where $\hat{n}_{d_\rho}$ is the d-boson number operator for neutron (proton), as

$$\hat{n}_{d_\rho} = d^\dagger \cdot \tilde{d}; \quad \tilde{d}_{\rho m} = (-1)^m d_{\rho,-m}, \tag{11}$$

then, $s^\dagger_\rho$, $d^\dagger_{\rho m}$ and $s_\rho$, $d_{\rho m}$ are the s and d-boson creation and annihilation operators. The neutron and proton are designated by $\nu$ and $\pi$, respectively. The $s_\pi$, $s_\nu$, $d_\pi$, and $d_\nu$ specify proton and neutron bosons with $L = 0, 2$, respectively.

The additional operators in Eq. (7) are defined as follows [2]:

$$Q_\rho = \left(d^\dagger \times s + s^\dagger \times \tilde{d}\right)^2_\rho + \chi_\rho \left(d^\dagger \times \tilde{d}\right)^2_\rho, \tag{12}$$

$$\hat{V}_{\rho\rho} = \sum_{k=1,2,4} \frac{1}{2} (2L+1)^{1/2} C^\rho_L \left[\left(d^\dagger_\rho \times d^\dagger_\rho\right)^{(L)} \cdot \left(\tilde{d}_\rho \times \tilde{d}_\rho\right)^{(L)}\right]^{(0)}, \tag{13}$$

$$\begin{aligned} M_{\pi\nu} = {} & \xi_2 \left(s^\dagger_\nu \times \tilde{d}_\pi - \tilde{d}_\nu \times s^\dagger_\pi\right)^{(2)} \cdot \left(s_\nu \times d^\dagger_\pi - d^\dagger_\nu \times s_\pi\right)^{(2)} \\ & - 2 \sum_{k=1,3} \xi_k \left(d^\dagger_\nu \times d^\dagger_\pi\right)^{(k)} \cdot \left(\tilde{d}_\nu \times \tilde{d}_\pi\right)^{(k)}. \end{aligned} \tag{14}$$

Consequently, it is also possible to analyze electromagnetic transitions within the IBM-2 framework; the E2 transition operator is stated [28, 29]:

$$T(E2) = e_\rho \left(d^\dagger_\rho s + s^\dagger_\rho \tilde{d}\right)^{(2)} + \chi_\rho \left(d^\dagger_\rho \tilde{d}_\rho\right)^{(2)}, \tag{15}$$

$\chi_\rho$ represents a dimension coefficient, while $e_\rho$ indicates the effective quadrupole charge. The $B(E2)$ operator in the IBM-2 model can also be defined as [28]:

$$T(E2) = e_\pi Q_\pi + e_\nu Q_\nu, \tag{16}$$

where $Q_\rho$ is the quadrupole operator. $e_\pi$ and $e_\nu$ are boson effective charges.

## Results and Deliberations

We describe the excitation spectra of ground states, $\gamma$, and $\beta$ bands of the $^{182}$Hg and $^{184}$Hg isotopes. The fitting approach attempts to achieve the best agreement with experimental data, including ground states, $\gamma$, and $\beta$ band energies and $B(E2)$ for $^{182,184}$Hg. The $\varepsilon$, $a_0$, $a_1$, $a_2$, $a_3$, $a_4$, and $a_5$ parameters (see Table 1) can be calculated by diagonalizing Eq. 1 in a complete basis. The symbol $a_0$, $a_1$, $a_2$, $a_3$, and $a_4$ are the limits for designating the $\hat{P}$, $\hat{L}$, $\hat{Q}$, and $\hat{T}_r$. The $\varepsilon = \text{EPS}$, $a_0 = 2\text{PAIR}$, $a_1 = \text{ELL}/2$, and $a_3 = 5\text{OCT}, \text{CHI} = 0$ are PHITS parameters [25]. The energy levels are calculated using the NPBOS code [30].

| *Nucl.* | $\epsilon$ | $a_0$ | $a_1$ | $a_2$ | $a_3$ | $a_4$ | CHQ ($\chi$) |
|---|---|---|---|---|---|---|---|
| $^{182}$Hg | 0.000 | 0.000 | 0.0057 | –0.0031 | 0.000 | 0.000 | -1.333 |
| $^{184}$Hg | 0.25 | 0.000 | 0.0280 | –0.0024 | 0.2159 | 0.000 | -1.333 |

TABLE 1. *IBM-1 parameters. All parameters are given in MeV, except N and CHQ ($\chi$)*

The Hamiltonian (Eq.10) was diagonalized to compute the parameters $\varepsilon_d$, $\kappa$, $\chi_\pi$, $\chi_\nu$ and $C_L$ (see Table 2) for suitable acceptable measured data. When the interactions between protons ($V_{\pi\pi}$) and between neutrons ($V_{\nu\nu}$) are added up, the coefficients $C_L$ are designated as $C_L^\nu(N_\nu)$ and $C_L^\pi(N_\pi)$. Then, the proton-proton interaction is determined from the number of proton bosons ($N_\pi$), while the neutron-neutron interaction is determined from the number of neutron bosons ($N_\nu$). In this study, $^{208}$Pb is involved as an inert core to compute the number of bosons in nuclei. The valence nucleons are calculated from the double magic nucleus $^{208}$Pb ($Z = 82, N = 126$). $^{182}$Hg and $^{184}$Hg nuclei belong near the shell closure of $^{208}$Pb; there are 2 holes that exist due to a shortage of valence protons in the shell closure of magic number $Z = 82$ and 24 holes, and 22 holes exist due to a shortage of neutrons in the shell closure of magic number $N = 126$. Therefore, the total number of bosons ($N$) in $^{182}$Hg and $^{184}$Hg is 11 and 12, respectively.

| *Nucl.* | $\epsilon_d$ | $\kappa_{\nu\pi}$ | $\chi_\pi$ | $\chi_\nu$ | $\xi_2$ | $C_0 L\pi$ | $C_0 L\nu$ |
|---|---|---|---|---|---|---|---|
| | | | | | | 2 | 2 |
| | | | | | | 4 | 4 |
| $^{182,184}$Hg | 0.550 | -0.160 | -0.080 | 0.200 | 0.030 | 0.000 | 0.250 |
| | | | | | | 0.000 | -0.070 |
| | | | | | | 0.000 | 0.110 |

TABLE 2. *IBM-2 parameters. All parameters are given in MeV*

The $R_{4/2} = \frac{E(4_1^+)}{E(2_1^+)}$ ratio can be used to divide the energies of nuclei into three distinct groups. The $R_{4/2}$ values for $^{182,184}$Hg isotopes of previously measured data [31–33], IBM-1, and IBM-2 are shown in Fig. 1. It is clear that the data from IBM-1 calculations are more consistently represented than those of IBM-2. The energy levels calculated from IBM-1 and IBM-2 for the ground and various states of the Hg isotopes are depicted in Fig. 2.

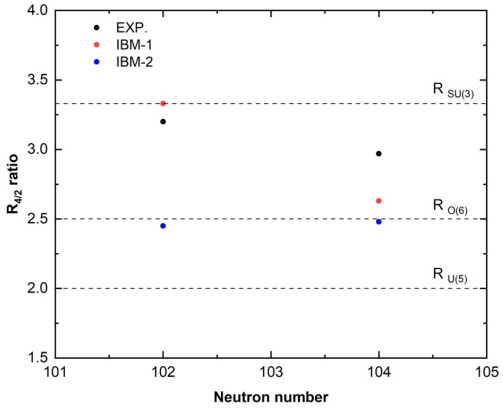


FIGURE 1. *$R_{4/2}$ ratio versus neutron number. The U(5), O(6), and SU(3) limits are represented in dashed lines. Black, red, and blue colors, respectively, indicate the results of previous experiments, IBM-1 and IBM-2*

The first look at the energy level structures of $^{182,184}$Hg nuclei shows that the experimental data, IBM-1 and IBM-2 are similar to each other compared to the experimental results. However, we may make multiple predictions. IBM-1 and IBM-2 correctly reflect the experimental energy levels of $0_1^+$ and $2_1^+$ states in the ground state of the $^{182,184}$Hg isotopes. For the $4_1^+$ state, the IBM-2 calculations are underestimated for $^{182,184}$Hg isotopes compared to the IBM-1, which represents exactly the same experimental value. However, IBM-2, in contrast to IBM-1, more precisely represents higher states, particularly $6_1^+$ and $8_1^+$.

The IBM-1 prediction accurately describes the energy levels in the $2_2^+$ states at $^{182,184}$Hg for the $\gamma$-bands, in contrast to the IBM-2 description. However, both IBM-1 and IBM-2 exhibit significant enhancements for high states (e.g., $4_2^+$ and $5_1^+$). In IBM-2 calculations, there exists a small gap between the $3_1^+$ and $5_1^+$ states in the $^{182,184}$Hg configuration. The energy levels for all $\beta$-states were not accurately represented in the IBM-2 calculations for $^{182,184}$Hg isotopes. On the contrary, the IBM-1 model only accurately represents the $0_2^+$ state in $^{184}$Hg isotope and underestimates the same state in $^{182}$Hg isotope. IBM-1 significantly underrepresents the higher states.

Furthermore, our calculations were compared with previous studies (an interacting boson model with configuration mixing (IBM-CM) [35], a beyond

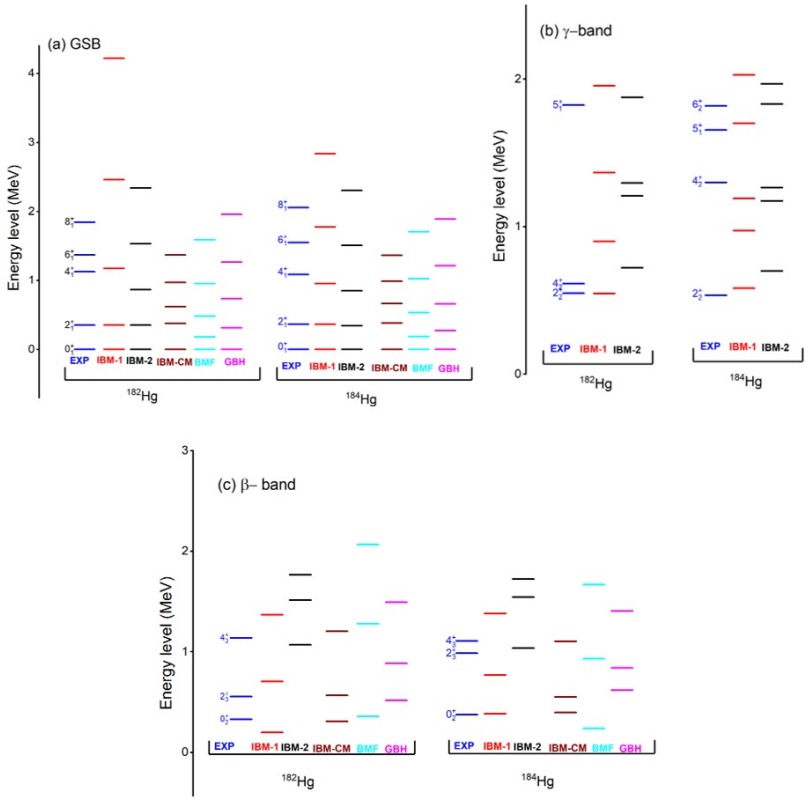


FIGURE 2. *Experimental data [31, 34], IBM-1, IBM-2, IBM-CM [35], BMF [36], and GBH [37] energy level results for (a) g, (b) $\gamma$, and (c) $\beta$ bands in $^{182}Hg$ and $^{184}Hg$ isotopes*

mean-field model (BMF) [36], and the General Bohr Hamiltonian (GBH) [31, 34, 37–40]) as presented in Fig. 2. Relative to the BMF and GBH calculations, which did not employ fitting parameters, the IBM-CM calculations used nine fitting parameters for each isotope, which means the calculations more closely match the experimental data. Irrespective of all the computations in the GS band, the IBM-2 calculations for the $^{182}$Hg had the smallest RMS error (root mean square deviation). In contrast to other theoretical calculations, the IBM-1 is precisely represented in the experimental data for $^{184}$Hg in the GS band with a small error. Moreover, IBM-1 had less error in both of the selected nuclei for the $\gamma$ band. For the $^{182}$Hg isotope, the IBM-CM approach fits experimental data well in the $\beta$ band, while the IBM-1 has a lower error in representing the data for the $^{184}$Hg isotope.

For B(E2) values, we selected to match the calculated absolute strengths of transitions within the ground state band with experimental values. In order to

determine the effective charge ($\alpha_2$) in IBM-I, experimental data $B(E2; 2_1^+ \rightarrow 0_1^+)$ for each isotope is normalized using Eq. 13. The value of parameter $\alpha_2^2$ for each isotope is calculated from the given measured value of transitions $(2_1^+ \rightarrow 0_1^+)$ and used to calculate $B(E2)$ values.

Our study focuses primarily on the $E2$ transitions, which are an essential part of the collective nuclear structure. The fitting of $B(E2 : 2_1^+ \rightarrow 0_1^+)$ to the measured data can be used to calculate the $e_\pi$ and $e_\nu$ values. The wave functions are estimated by diagonalizing the IBM-2 Hamiltonian, and the electromagnetic transition was estimated using the program NPBEM [30]. IBM-1, IBM-2, and previous experimental data are presented in Table 3. Our calculation for both IBM-1 and IBM-2 overestimates the experimental $E2$ transition sequence for the $^{182,184}$Hg bands, except for $B(E2; 2_1^+ \rightarrow 0_1^+)$. The interband transition exhibits a significant variation from the empirical data. The experimental transition strength of $B(E2; 4_1^+ \rightarrow 2_1^+)$ to the corresponding experimental value of $B(E2; 2_1^+ \rightarrow 0_1^+)$ is notably large. This indicates that the various configurations were strongly mixed.

| **Nucl.** | $\alpha$ **(eb)** | $\beta$ **(eb)** | $J_i \rightarrow J_f$ | **Exp. [31, 34]** | **IBM-1** | **IBM-2** | **IBM-CM [35]** | **BMF [36]** | **GBH [37]** |
|---|---|---|---|---|---|---|---|---|---|
| | | | $2_1^+ \rightarrow 0_1^+$ | 0.33(2) | 0.33 | 0.50 | 0.34 | 1.68 | 0.88 |
| | | | $4_1^+ \rightarrow 2_1^+$ | 1.52(5) | 0.47 | 0.78 | 1.6 | 2.51 | 1.80 |
| | | | $6_1^+ \rightarrow 4_1^+$ | 2.27(18) | 0.50 | 0.96 | 2.07 | 2.98 | 2.29 |
| $^{182}$Hg | 0.078 | -0.2315 | $8_1^+ \rightarrow 6_1^+$ | 2.33(25) | 0.49 | 1.07 | 2.17 | 3.27 | 2.64 |
| | | | $10_1^+ \rightarrow 8_1^+$ | 2.45(61) | 0.47 | 1.42 | 2.18 | 3.55 | 2.94 |
| | | | $2_2^+ \rightarrow 2_1^+$ | 0.80(24) | 0.48 | 0.51 | 0.6 | 0.015 | 0.56 |
| | | | $4_1^+ \rightarrow 2_2^+$ | 1.20(3) | 0.34 | 0.00 | 0.25 | 0.015 | 0.05 |
| | | | $2_1^+ \rightarrow 0_1^+$ | 0.47(15) | 0.4802 | 0.5640 | 0.39 | 1.31 | 1.02 |
| | | | $4_1^+ \rightarrow 2_1^+$ | 1.22(4) | 0.92 | 0.88 | 1.09 | 2.37 | 1.82 |
| | | | $6_1^+ \rightarrow 4_1^+$ | 1.92(9) | 1.27 | 1.09 | 1.8 | 2.74 | 2.27 |
| $^{184}$Hg | 0.176 | -0.012 | $8_1^+ \rightarrow 6_1^+$ | 1.92(8) | 1.53 | 1.23 | 1.9 | 3.05 | 3.76 |
| | | | $2_2^+ \rightarrow 2_1^+$ | 0.54(0.08) | 0.67 | 0.43 | 0.83 | 0.78 | 0.53 |
| | | | $4_1^+ \rightarrow 2_2^+$ | [1.0] | 0.06 | 0.00 | 0.49 | 0.01 | 0.025 |

TABLE 3. *$B(E2)_\downarrow$ results for $^{182,184}$Hg nuclei, where $e_\pi = 0.167$ and $e_\nu = 0.184$ in the IBM-2*

Our calculations indicate that the interband transition is insignificant, suggesting that the mixing effect is not substantial in IBM-1 and IBM-2 calculations. This observation may have significance regarding the expected level of structure. The weak $E2$ transition is resulting from the second band consistently exceeding those of the ground-state band. This discrepancy appears to have the same cause as in $^{184}$Hg. Moreover, the present calculations are also compared with previous studies [35–37]. This comparison shows that the calculated $B(E2)$ by IBM-2 is better than those of previous studies. Moreover, the BMF and GBH calculations indicate overestimated values of

$B(E2)$ compared to experimental data. Overestimating the current deformation at the mean-field level could be the cause.

When comparing results of the IBM-CM model, it is evident that the experimental data is well reproduced. It should be noted that the IBM-CM approach used nine parameters to fit the experimental data. The IBM-CM model exceeds the BMF, GBH, IBM-1, and IBM-2 for a good reproduction of the experimental data. The structural change is therefore rapid, based on the IBM-CM results; however, the other theoretical calculations tend to show a small change between the transition groups. Then, the interband transition strength in the theoretical calculations must be corrected to perfectly match experimental results.

The experimentally and theoretically $B_{4/2}$ results are presented together in Fig. 3. The IBM-CM theoretical calculations and the experimental $B_{4/2}$ ratio for $^{182,184}$Hg nuclei are compatible, but the other theoretical calculations poorly represent the experimental results. Furthermore, it is essential to point out that the $2_1^+$ states of these nuclei exhibit the predicted correlates between the $B_{4/2}$ and $R_{4/2}$ ratios.

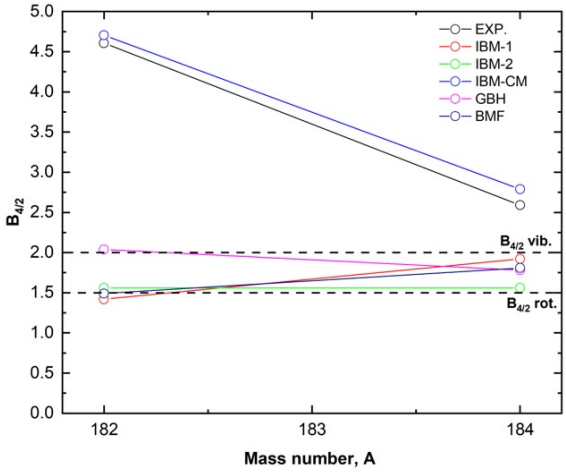


FIGURE 3. *The $B_{4/2}$ ratio for $^{182,184}$Hg isotopes*

The analysis of the potential energy surface (PES) can reveal the structure of $^{182,184}$Hg. The asymmetry in the nucleus is distinguished by the $\gamma$ term: a prolate nucleus is represented by $\gamma = 0°$, whereas an oblate nucleus is denoted by $\gamma = 60°$. The prolate shape of the energy surfaces for $^{182}$Hg is more pronounced, whereas the oblate shape gradually decreases in energy as it reaches $^{184}$Hg (displays a $\gamma$-soft transition). The PES contour of $^{182,184}$Hg is shown in Fig. 4.

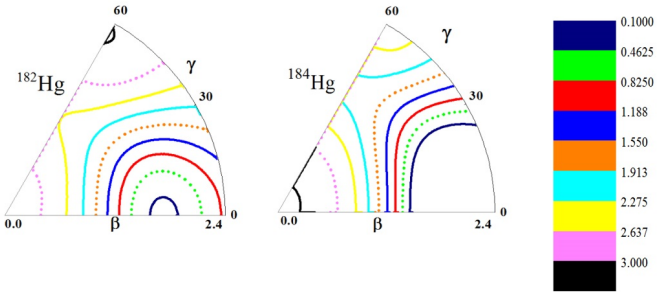


FIGURE 4. *The PES contour of* $^{182,184}$*Hg*

## Conclusions

Theoretical calculations employed IBM-1 and IBM-2 for $^{182,184}$Hg isotopes to calculate g-band, $\beta$-band, $\gamma$-band, and B(E2) were compared to experimental data. The $0^+$ and $2^+$ state results given in IBM-1 and IBM-2 indicate the differences between these configuration types in ground state bands. Both theoretical calculations give a different energy gap for higher spin states (i.e., $J = 4^+, 6^+, 8^+$) because of the overlap of the intruder states with energy levels.

The IBM-1 prediction accurately describes the energy levels in the $2_2^+$ states at $^{182,184}$Hg for the $\gamma$-bands, in contrast to the IBM-2 description. However, both IBM-1 and IBM-2 exhibit significant enhancements for high states. The energy levels for all $\beta$-states were not accurately represented in the IBM-2 calculations for $^{182,184}$Hg isotopes. On the contrary, the IBM-1 model only accurately represents the $0_2^+$ state in $^{184}$Hg isotope and underestimates the same state in $^{182}$Hg isotope. IBM-1 significantly underrepresents the higher states.

The IBM-CM calculations included nine fitting parameters for each isotope, resulting in a more accurate match to experimental results than theoretical computations. The IBM-1 and IBM-2 contribute a good estimate for $B(E2;2_1^+ \rightarrow 0_1^+)$, but for larger transitions, both calculations fail to match well the experimental data. This suggests a considerable mixing of the different configurations. The interband transition is negligible, according to our estimates, indicating that the mixing impact is not relevant in IBM-1 and IBM-2 computations. The weak E2 transition is resulting from the second band consistently exceeding those of the ground-state band. However, only the IBM-CM approaches calculate the B(E2) very well. The IBM-CM theoretical approach accurately illustrates the $B_{4/2}$ ratio for $^{182,184}$Hg compared to other calculations. The $R_{4/2}$ ratio shows that the $^{182,184}$Hg experiences an SU(3)-O(6) transition, which is consistent with EPS predictions. The IBM-1 model is superior and more straightforward than the IBM-2 model in EPS calculations.

## Acknowledgments

We acknowledge our thanks to the University of Alkafeel and University of Mosul for their invaluable assistance throughout this research. The authors express their gratitude to Prof. Dr. Hayder Al Mousawy, Ph.D., in English for editing the English language of this work.

## References

[1] A. Arima and et al., Phys. Lett. B **66**, 205 (1977).
[2] T. Otsuka, , and et al., Phys. Lett. B **76**, 139 (1978).
[3] G. L. Long and et al., J. Phys. G: Nucl. Part. Phys. **21**, 331 (1995).
[4] F. Iachello, Phys. Rev. Lett. **87**, 052502 (2001).
[5] A. Sevrin, K. Heyde, and J. Jolie, Phys. Rev. C **36**, 2621 (1987).
[6] M. A. Al-Jubbori and et al., Chinese Phys. C **41**, 084103 (2016).
[7] K. Heyde, J. Jolie, and et al., Nucl. Phys. A **586**, 1 (1995).
[8] M. Al-Jubbori and et al., Indian J. Phys. **94**, 379 (2020).
[9] R. Julin and et al., J. Phys. G: Nucl. Part. Phys. **27**, R109 (2001).
[10] M. Siciliano and et al., Phys. Rev. C **102**, 014318 (2020).
[11] V. V. Prassa and K. Karakatsanis, Bulg. J. Phys. **48**, 495 (2021).
[12] J. García-Ramos and K. Heyde, EPJ Web Conf. **93**, 01004 (2015).
[13] M. A. Al-Jubbori, Ukr. J. Phys. **62**, 936 (2017).
[14] H. T. Fortune, Phys. Rev. C **100**, 044303 (2019).
[15] M. Stryjczyk and et al., Phys. Rev. C **108**, 014308 (2023).
[16] F. Iachello and A. Arima, *The Interacting Boson Model* (Cambrige University, 1987).
[17] A. M. Al-Nuaimi and et al., KIJOMS **8**, 391 (2022).
[18] H. H. Kassim and et al., Momento **69**, 101 (2024).
[19] A. Arima and F. Iachello, Ann. Phys. **111**, 201 (1978).
[20] M. A. Al-Jubbori and et al., Int. J. Mod. Phys. E **27**, 1850035 (2018).
[21] H. H. Khudher and et al., Ukr. J. Phys. **62**, 152 (2017).
[22] A. Arima and F. Iachello, Ann. Phys. **99**, 253 (1976).
[23] F. Iachello, Phys. Rev. Lett. **44**, 772 (1980).
[24] A. Mohammed-Ali and et al., Rev. Mex. Fís. **68**, 060401 1 (2022).
[25] I. Mamdouh and M. Al-Jubbori, Indian J. Phys. **89**, 1085 (2015).
[26] S. Nair, A. Ansari, and L. Satpathy, Phys. Lett. B **71**, 257 (1977).
[27] F. M. Ali and et al., Momento **68**, 86 (2024).
[28] G. Puddu, O. Scholten, and T. Otsuka, Nucl. Phys. A **348**, 109 (1980).
[29] M. A. Al-Jubbori and et al., Phys. Atom. Nuclei **82**, 201 (2019).

[30] T. Otsuka and N. Yoshida, User's manual of the program NPBOS. Report JAERI-M 85-094 (1985).

[31] National Nuclear Data Center. Brookhaven National Laboratory (Consulted in 2024).

[32] B. Singh, Nucl. Data Sheets **130**, 21 (2015).

[33] C. M. Baglin, Nucl. Data Sheets **111**, 275 (2010).

[34] J. Batchelder, A. Hurst, and M. Basunia, Nucl. Data Sheets **183**, 1 (2022).

[35] J. E. García-Ramos and K. Heyde, Phys. Rev. C **89**, 014306 (2014).

[36] J. M. Yao, M. Bender, and P.-H. Heenen, Phys. Rev. C **87**, 034322 (2013).

[37] L. Próchniak and S. G. Rohoziński, J. Phys. G: Nucl. Part. Phys. **36**, 123101 (2009).

[38] M. Najem and M. Al-Jubbori, J. Educ. Sci. **30**, 175 (2021).

[39] F. Ali, M. Al-Jubbori, and A. Elbndaq, J. Educ. Sci. **32**, 1 (2023).

[40] M. Yousif, J. Educ. Sci. **33**, 74 (2024).